Multistage adsorption of diffusing macromolecules and viruses

Tom Chou[1,2] and Maria R. D'Orsogna[2]

[1]Dept. of Biomathematics, UCLA, Los Angeles, CA 90095-1766
[2]Dept. of Mathematics, UCLA, Los Angeles, CA 90095-1555
(Dated: February 6, 2008)

We derive the equations that describe adsorption of diffusing particles onto a surface followed by additional surface kinetic steps before being transported across the interface. Multistage surface kinetics occurs during membrane protein insertion, cell signaling, and the infection of cells by virus particles. For example, viral entry into healthy cells is possible only after a series of receptor and coreceptor binding events occur at the cellular surface. We couple the diffusion of particles in the bulk phase with the multistage surface kinetics and derive an effective, integro-differential boundary condition that contains a memory kernel embodying the delay induced by the surface reactions. This boundary condition takes the form of a singular perturbation problem in the limit where particle-surface interactions are short-ranged. Moreover, depending on the surface kinetics, the delay kernel induces a nonmonotonic, transient replenishment of the bulk particle concentration near the interface. The approach generalizes that of Ward and Tordai [1] and Diamant and Andelman [2] to include surface kinetics, giving rise to qualitatively new behaviors. Our analysis suggests a simple scheme by which stochastic surface reactions may be coupled to deterministic bulk diffusion.

PACS numbers: 68.43.+h, 87.68.+z, 68.47.Pe, 68.03.+g

I. INTRODUCTION

The kinetics of surface particle adsorption and of transport through interfaces play a key role in surfactant phenomena [3, 4], membrane biology and cell signaling [5–10], marine layer oceanography [11], and other biological and chemical processes. Particle adsorption may fundamentally alter the physical and chemical properties of the interface, and it is crucial to understand both equilibrium and dynamical properties of the adsorbed layers [1, 3, 4, 6]. In the seminal work of Ward and Tordai [1], a bulk phase acting as a reservoir of particles is physically limited by an empty surface onto which the particles can adsorb. Particles are assumed to lower their free energy with respect to the bulk phase by irreversibly and instantaneously adsorbing onto the interface. Under these conditions, the total concentration of adsorbed particles may be estimated in relation to measurable interfacial properties, such as the dynamic surface tension. Several applications, extensions and alternate approaches to this work have been proposed [2, 12]. In particular, adsorption dynamics in the Ward-Tordai setting can be rederived through a free energy approach [2], allowing for the inclusion of ionic surfactant effects and electrostatic interactions.

In many biochemical systems, the complete adsorption of a particle arriving from the bulk requires a series of auxiliary transformations at the surface before the particle can be successfully incorporated, or 'fused' into the surface. These intermediate steps gives rise to a lag-time in the complete adsorption process. For example, the incorporation of emulsify-

ing proteins onto an air-water interface may be delayed by the unfolding of the polypeptide at the interface [7]. Adsorption of proteins on polymer-grafted interfaces, such as the glycocalyx layer of vascular endothelial cells, is also delayed due to the progressive insertion of the protein through the polymer brush[13, 14] . Kinetic delays have also been observed in the adsorption of the hemagglutinin glycoprotein (HA) of the influenza virus as it enters target host cellular membranes [15]. The mechanisms underlying this delay are not known in detail but are believed to involve conformational changes of HA molecules into fusion enabling complexes, mediated by the presence of binding receptors and coreceptors on the target cell membrane [15–17]. Similarly, the incorporation of an HIV particle into a T-cell or a macrophage is possible only after the gp120 glycoprotein of the HIV virus membrane recognizes and binds to the target cell surface receptor CD4, and subsequently to other coreceptors such as CCR5 or CXCR4. As in the case of HA and influenza, the exact number of gp120-bound receptors and coreceptors required for HIV particle fusion is yet unknown and might depend on gp120 conformations and receptor/coreceptor binding cooperativity [18, 19]. The complex nature of surface biochemistry makes quantitative kinetic measurements challenging. Recently, the binding kinetics of the CD4 cellular receptor to the gp120 HIV ligand have been measured under different experimental conditions yielding widely different dissociation rates [20, 21]. In this work, we will provide a quantitative framework that can be used to better understand the experimentally observed lag-times in surface kinetics
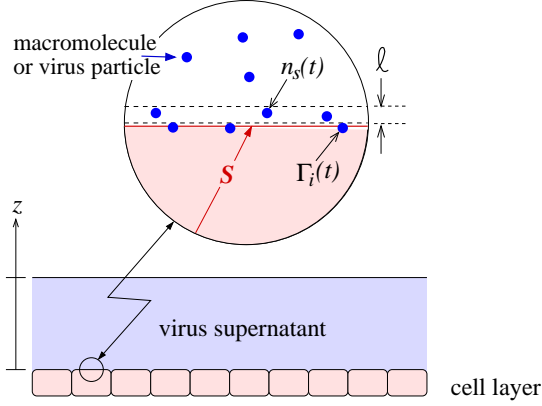
FIG. 1: A schematic of a typical adsorption experiment on a confluent monolayer of target cells. The location of the interface is labelled by **S**. Particles such as viruses are spread over the cell layer in a thin supernatant film. Inset: After initial nonspecific viral adsorption on the supernatant-cell interface, cellular receptors and coreceptors bind to the virus via a certain stoichiometry, forming fusion intermediates Γ_i. The subsurface layer of thickness ℓ, the subsurface concentration $n_s(t)$, and the adsorbed species $\Gamma_i(t)$ are discussed in the text.

phenomena that involve multistage surface chemistry.

In particular, we will explicitly consider intermediate, reversible steps for surface binding in the Ward-Tordai formalism, deriving an effective boundary condition to complement the bulk diffusion process. Chemical transitions among the surface species will introduce memory terms in the boundary conditions for the bulk concentration. Our analysis can be readily applied to the titration of replication-incompetent virus via a colony formation assay [22] as shown in Fig. 1.

II. MODEL EQUATIONS

In this section, we motivate and derive the equations coupling bulk diffusion to surface layer evolution. We consider a general, linear reaction scheme to describe the multistep surface reaction dynamics. Effective boundary conditions for diffusion from the bulk are derived in Sect. 3. As we shall discuss in detail, we are able to embody the response of the adsorbing particle system to the existence of intermediate chemical steps at the surface, into a unique delay kernel regulating the boundary dynamics. All microscopic details stemming from the surface dynamics, no matter how complicated, are contained in the derived memory kernel. Our approach includes ligand rebinding to surfaces, found to be important for analyzing surface plasmon resonance assays of bio-

chemical systems [23]. In Sect. 4 we particularize our surface reaction scheme to a specific Markov process chain and evaluate all physically relevant quantities.

A. Bulk Diffusion

In the continuum limit, the density of particles $n(\mathbf{r}, t)$ in the bulk phase obeys the convection-diffusion equation

$$\frac{\partial n}{\partial t} = \nabla \cdot [D \nabla n] + \frac{1}{k_B T} \nabla \cdot [D\, n \nabla U], \qquad (1)$$

where $D(\mathbf{r})$ and $U(\mathbf{r})$ are the local diffusion coefficient and potential of mean force, respectively, and $k_B T$ is the thermal energy. Spatial variation of $D(\mathbf{r})$ and $U(\mathbf{r})$ may arise from interactions with the interface as shown in Fig. 3. Boundary conditions are typically applied at the mathematical surface onto which the particles adsorb or reflect. By balancing the diffusive flux just above this mathematical interface with the particle rate of insertion into the interface, a mixed boundary condition arises

$$D(\mathbf{r})\, \hat{\mathbf{n}} \cdot \nabla n(\mathbf{r}, t) = \gamma n(\mathbf{r}, t), \quad \mathbf{r} \in \mathbf{S}. \qquad (2)$$

Here, **S** denotes the substrate; its normal direction is $\hat{\mathbf{n}}$. The parameter γ, which has the physical units of speed, is proportional the probability f (often called the accommodation coefficient [24] or sticking probability [25, 26]) that a particle is adsorbed into the mathematical interface upon collision. We define $\gamma = \gamma_0 f$ such that in the limit $\gamma_0 \to \infty$ and $f \neq 0$, Eq. 2 is equivalent to $n(\mathbf{r} \in \mathbf{S}) = 0$, an absorbing boundary condition. A reflecting boundary condition, $\hat{\mathbf{n}} \cdot \nabla n = 0$, arises when $f = 0$. Equations 1 and 2 are commonly used to model simple diffusion-adsorption processes at surfaces.

B. Surface Reactions

In many applications, particles at an interface undergo chemical or physical modifications that control for example, surface reactivity, surface tension [1–4], and conductivity [25]. Biological examples include tissue factor initiated coagulation reactions and viral entry. Coagulation factors must work their way through the glycocalyx layer before they can be enzymatically primed by the membrane-bound tissue factors [27]. Entry of viruses, such as HIV, into cells require the binding of membrane-bound receptors and coreceptors before fusion with the target cell can occur. All of these processes can be thought of as reactions at the membrane surface. Immediately
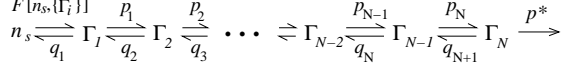
3

$$F[n_s,\{\Gamma_i\}]$$
$$n_s \underset{q_1}{\overset{}{\rightleftharpoons}} \Gamma_1 \underset{q_2}{\overset{p_1}{\rightleftharpoons}} \Gamma_2 \underset{q_3}{\overset{p_2}{\rightleftharpoons}} \cdots \rightleftharpoons \Gamma_{N-2} \underset{q_N}{\overset{p_{N-1}}{\rightleftharpoons}} \Gamma_{N-1} \underset{q_{N+1}}{\overset{p_N}{\rightleftharpoons}} \Gamma_N \overset{p^*}{\longrightarrow}$$

FIG. 2: Surface reaction scheme among the intermediate states Γ_i. The source species Γ_1 is supplied by the bulk surface concentration at the interface, n_s. In the context of virus recognition and infection, the intermediate steps label various numbers of receptors or coreceptors associated with the surface bound virus particle. For example, Γ_i may denote the surface concentration of HIV particles with i receptors and coreceptors attached. This catenary model could also represent successive degrees of insertion of an absorbing species through a polymer brush or glycocalyx coated interface.

after adsorption from the bulk, the surface particle concentration, whether of coagulation factors or of virus particles, is denoted by Γ_1. For example, in the case of viruses, we can identify the Γ_1 state as being that of a virus bound to $i = 1$ CD4 surface receptor. The initially adsorbed species can then kinetically evolve into the other species Γ_i representing virus particles with $i > 1$ bound receptors or coreceptors. The kinetics among the N surface species follows the linear rate equation $\partial_t \boldsymbol{\Gamma} = \mathbf{M}\boldsymbol{\Gamma} + \mathbf{F}(t)$, where $\boldsymbol{\Gamma} \equiv (\Gamma_1, \Gamma_2, \ldots, \Gamma_N)$, $\mathbf{M}$ is the transition matrix among the N surface states, and $\mathbf{F} \equiv (F, 0, \ldots, 0)$ is the source of the first, originating source species Γ_1 coming from the bulk.

Figure 2 illustrates a simple example of a linear surface reaction scheme that can be described by the above linear rate equation. In this case the reaction matrix $\mathbf{M}$ is tridiagonal. General reaction matrices can also be analyzed since our results depend only on the eigenvalues and eigenvectors of $\mathbf{M}$.

C. Surface Layer

Because the surface densities Γ_i carry units of number per area, and the bulk densities are expressed by number per volume, any kinetic parameter linking bulk source concentrations to those at the interface must introduce a physical length scale. Diamant and Andelman [2] have introduced the sublayer thickness as a mathematical step coupling the bulk density to surface density. Here, we physically motivate this "surface layer" and the associated transport. Let us thus introduce a thin layer of thickness ℓ near the surface, in which the particle density is denoted $n_s(t)$ and is still expressed in units of number per volume.

The continuum approximation Eq. 1 breaks down when resolving the transport within distances of a few mean free paths. If we identify the sublayer thickness ℓ with the mean free path ℓ_{mfp}, as shown in Fig. 3, we
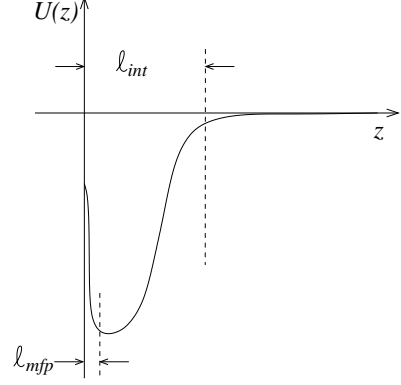

FIG. 3: Interaction potential between diffusing species and the interface. The subsurface layer is defined by either the range of the interaction potential ℓ_{int}, or the mean free path ℓ_{mfp}, depending upon which is larger.

must solve Eq. 1 with a nonuniform $U(\mathbf{r})$, and possibly a nonuniform $D(\mathbf{r})$, to within a distance $\ell = \ell_{mfp}$ of the interface. For the choice $\ell = \ell_{mfp}$, the adsorption velocity γ_0 can be approximated by the thermal velocity v_T such that $\gamma = \gamma_0 f \sim v_T f$. The value of the bulk density at the boundary $\mathbf{S} + \ell \hat{\mathbf{n}}$ is defined as the sublayer density: $n(\mathbf{r} = \mathbf{S} + \ell \hat{\mathbf{n}}, t) \equiv n_s(t)$. The equation for the rate of change of the number per area of molecules in the thin layer, $d(\ell n_s(t))/dt$ can be obtained by balancing the latter with the diffusive flux into the layer $D(\mathbf{r}) \hat{\mathbf{n}} \cdot \nabla n(\mathbf{S} + \ell \hat{\mathbf{n}}, t)$, the adsorption into the surface concentration Γ_1, and the spontaneous desorption from the initially adsorbed species Γ_1 occurring at rate q_1. The complete set of equations coupling the variables $n(\mathbf{r}, t), n_s(t)$, and Γ_i is thus

$$\frac{\partial n}{\partial t} = \nabla \cdot [D \nabla n] + \frac{1}{k_B T}\nabla \cdot [D n \nabla U], \quad (3)$$

$$\ell \frac{dn_s}{dt} = -F + D\,\hat{\mathbf{n}}\cdot\nabla n\Big|_{\mathbf{r}=\mathbf{S}+\ell\mathbf{n}} + q_1 \Gamma_1, \quad (4)$$

$$\frac{d\boldsymbol{\Gamma}}{dt} = \mathbf{M}\boldsymbol{\Gamma} + \mathbf{F}, \quad \mathbf{F} = (F, 0, 0, \ldots, 0). \quad (5)$$

Here, $n|_{\mathbf{r}=\mathbf{S}+\ell\mathbf{n}} = n_s$, and $F = F[n_s, \{\Gamma_i\}]$ is the flux of the surface concentration n_s into the incipiently adsorbed species Γ_1. This functional may depend on interactions among the adsorbed species Γ_i, including cooperative or crowding effects, and may be modeled using free energies and chemical potential differences between the bulk and surface [2, 13].

A further simplification can be introduced by defining a different sublayer thickness $\ell = \ell_{int}$, where ℓ_{int} is the typical range of the particle-surface interaction as shown in Fig. 3. In this case, at least at a distance ℓ_{int} from the interface, $D(\mathbf{r})$ is constant, $U(\mathbf{r})$ is zero

and Eq. 1 is approximated by the standard diffusion equation

$$\frac{\partial n(\mathbf{r}, t)}{\partial t} = D\nabla^2 n(\mathbf{r}, t). \qquad (6)$$

All effects of the potential of mean force $U(\mathbf{r})$ and spatially varying $D(\mathbf{r})$ are now subsumed into an effective source $F[n_s, \{\Gamma_i\}]$. This is consistent with all previous treatments [1, 2, 4] in which transport in the bulk phase was described by simple diffusion with uniform D and U. Provided $F[n_s, \Gamma_i]$ is independent of Γ_i, equations 1-5 can be explicitly solved in simple geometries. For low surface densities Γ_i such that additional adsorption is not hindered by steric exclusion, one can assume a form $F[n_s]$ independent of surface concentrations Γ_i. For $\ell = \ell_{int}$, γ is now interpreted as an effective adsorption coefficient allowing Eq. 1 to be replaced by Eq. 6, and simplifying the bulk concentration equation.

III. ANALYSIS

Following the original work of Ward and Tordai, subsequent studies on adsorption and dynamic surface tension measurements [1, 4] eliminate the bulk density at the interface in Eq. 4 to yield two coupled integro-differential equations for n_s and Γ_1 which must be numerically self-consistently solved. Here, we solve the linear Eqs. 5 independently from the bulk densities, but with a source term $F[n_s]$ that connects the surface concentrations Γ_i with the bulk concentration $n(\mathbf{r}, t)$. If $F[n_s]$ is independent of Γ_i, the explicit solution to Eqs. 5 can be found by evaluating the eigenvalues λ_j and corresponding eigenvectors $\mathbf{v}^j$ of the chemical transition matrix $\mathbf{M}$. Denoting the similarity transform matrix $V_{kj} \equiv v_k^j$ such that $\mathbf{VMV}^{-1} = \mathrm{diag}(\lambda_j)$, the surface densities are

$$\begin{aligned} \Gamma_k(t) &= \sum_{j,m=1}^{N} V_{kj}^{-1} V_{jm} \Gamma_m(0) e^{\lambda_j t} \\ &+ \sum_{j=1}^{N} V_{kj}^{-1} V_{j1} \int_0^t e^{\lambda_j(t-t')} F[n_s(t')] \mathrm{d}t', \end{aligned}$$

$$(7)$$

where $\mathbf{\Gamma}(0)$ are the intermediate surface concentrations at $t = 0$. If there are no spontaneous sources of the surface cell intermediates, all eigenvalues $\lambda_j < 0$. From Eq. 7, in the case $\mathbf{\Gamma}(0) = 0$, $\mathbf{\Gamma}(t)$ is proportional to $F[n_s(t)]$. Upon substituting $\Gamma_1(t)$

By setting $k = 1$ in Eq. 7, we substitute $\Gamma_1(t)$ into Eq. 4, and find a concise description of the diffusion-adsorption process:

$$\frac{\partial n(\mathbf{r}, t)}{\partial t} = D\nabla^2 n(\mathbf{r}, t), \qquad n(\mathbf{S} + \ell\mathbf{n}, t) = n_s(t), \quad (8)$$

$$\ell\frac{\mathrm{d}n_s(t)}{\mathrm{d}t} = D\hat{\mathbf{n}}\cdot\nabla n(\mathbf{r}, t)\Big|_{\mathbf{r}=\mathbf{S}+\ell\mathbf{n}} - \int_0^t K(t-t')F[n_s(t')]\mathrm{d}t',$$

$$(9)$$

$$K(t) = \delta(t) - q_1 \sum_{j=1}^{N} V_{1j}^{-1} V_{j1} e^{\lambda_j t}, \qquad (10)$$

where $K(t)$ is the kernel constructed from the eigenvalues and eigenvectors of $\mathbf{M}$. It is composed of an instantaneous response – the immediate depletion of n_s due to adsorption into the Γ_1 surface species – and delay terms arising from the surface kinetics of Eq. 5. The complete set of equations 8-10 is one of our main findings. This result explicitly shows how multistage adsorption is modeled by a bulk diffusion equation with an nonlinear integro-differential boundary condition that incorporates the delay arising from the multistep kinetics. Under this scheme, all effects of surface reactions are incorporated in the kernel $K(t)$.

Our analysis can be carried further by specifying a linear form for the Γ_i-independent source term

$$F[n_s(t)] = \gamma n_s(t), \qquad (11)$$

which simply takes the source for the surface concentration Γ_1 of the first species to be proportional to the subsurface concentration. The surfaces densities $\Gamma_i(t)$ can be found by substituting $n_s(t)$, derived from Eq. 8-10, into the expression for $F[n_s(t)]$ in Eq. 7. Note that the boundary condition Eq. 9 contains a singular perturbation, and that for times $t \gg \ell/\gamma$, the "outer solution" approximation $\ell(\mathrm{d}n_s/\mathrm{d}t) \approx 0$ yields the standard mixed boundary condition Eq. 2 with an additional memory kernel. Moreover, in the linear approximation of Eq. 11, the convolution of the delay term in the effective boundary condition 9 is amenable to analysis by Laplace transforms.

For simplicity, we will assume a simple one-dimensional problem where all quantities vary spatially only in the direction normal to an infinite, flat interface at $z = 0$. We nondimensionalize all quantities by using ℓ as the unit of length, and q_1^{-1} as the unit of time. Henceforth, in all equations, we make the replacements $z \to \bar{z}/\ell$, $t \to q_1\bar{t}$, $n \to \ell^3\bar{n}$, $n_s \to \ell^3\bar{n}_s$, $\Gamma_i \to \ell^2 \bar{G}_i$, $D \to \ell^{-2}\bar{D}/q_1$, and $\gamma \to \bar{\gamma}/(\ell q_1)$. To render the notation less cumbersome we omit the bars from the redefined quantities. In the discussion that follows, the $z, t, n, n_s, \Gamma_i, D, \gamma$ parameters are intended as nondimensional. Upon taking the

Laplace transform in time of the dimensionless forms of Eqs. 8, 9, and 10, we obtain

$$s\tilde{n}(z,s) - n_0 = D\partial_z^2 \tilde{n}(z,s), \qquad (12)$$

$$s\tilde{n}_s(s) - n_0 = D\partial_z \tilde{n}(z,s)\Big|_{z=1} - \gamma\tilde{K}(s)\tilde{n}_s(s), \quad (13)$$

where

$$\tilde{K}(s) = 1 - \sum_{j=1}^{N} \frac{V_{1j}^{-1} V_{j1}}{s - \lambda_j}, \qquad (14)$$

and n_0 is the initial, dimensionless constant bulk and sublayer concentration. The general solution to the bulk density $\tilde{n}(z,s)$ from Eq. 12 is

$$\frac{\tilde{n}(z,s)}{n_0} = \frac{1}{s} - \frac{\gamma\tilde{K}(s)\exp\left(-(z-1)\sqrt{s/D}\right)}{s(s + \sqrt{sD} + \gamma\tilde{K}(s))}. \quad (15)$$

Once the bulk density is derived, all other quantities can be found by inverse Laplace transforming $\tilde{n}(z,s)$. In the absence of spontaneous sources of the surface intermediates, $\lambda_j < 0$. In this case, it is possible to show that $\tilde{n}(s,z)$ only has a simple pole at $s = 0$ and a branch cut on $s = (-\infty, 0]$. Performing the integral along the latter, we find the exact results

$$n(z,t) = n_0 \int_0^\infty L(z,u)e^{-ut}\mathrm{d}u, \qquad (16)$$

and

$$\Gamma_k(t) = \gamma n_0 \sum_{j=1}^{N} V_{kj}^{-1} V_{j1} \int_0^\infty \frac{e^{\lambda_j t} - e^{-ut}}{u + \lambda_j} L(1,u)\mathrm{d}u, \qquad (17)$$

where

$$L(z,u) \equiv -\frac{\gamma}{\pi} \frac{(u - \gamma\tilde{K}(-u))\sin\sqrt{\frac{u}{D}}(z-1) - \sqrt{uD}\cos\sqrt{\frac{u}{D}}(z-1)}{u(u - \gamma\tilde{K}(-u))^2 + Du^2}\tilde{K}(-u). \qquad (18)$$

Equations 16-18 are used to numerically compute all of our results in the next Section. For completeness, analytic expressions for asymptotically short and long time limits are derived in the Appendix.

IV. RESULTS

We now specify a surface reaction scheme and construct its delay kernel by using its associated eigenvalues and eigenvectors. For applications such as multiple receptor binding of the adsorbed species, we consider a reversible sequential Markov process among N chemical intermediates Γ_i, $i = 1, \ldots, N$. As shown in Fig. 2, formation of state Γ_{i+1} from state Γ_i occurs at rate p_i, while the reverse step occurs at rate q_{i+1}. The final state Γ_N is irreversibly annihilated, by transport across the membrane, or by irreversible reaction, with rate p^*. We can then explicitly write the dimensional form of Eq. 5, where $\mathbf{M}$ is a tridiagonal transition matrix, as

$$\frac{\mathrm{d}\Gamma_1}{\mathrm{d}t} = F[n_s, \{\Gamma_i\}] - (p_1 + q_1)\Gamma_1 + q_2\Gamma_2,$$

$$\frac{\mathrm{d}\Gamma_i}{\mathrm{d}t} = p_{i-1}\Gamma_{i-1} - (q_i + p_i)\Gamma_i + q_{i+1}\Gamma_{i+1} \quad 2 \le i \le N-1$$

$$\frac{\mathrm{d}\Gamma_N}{\mathrm{d}t} = -(p^* + q_N)\Gamma_N + p_{N-1}\Gamma_{N-1}.$$

(19)

In the simplest case where there is only one surface intermediate before transport across the interface, $N = 1$ and the dimensionless ($q_1 = 1$) delay kernel is simply $\tilde{K}(s) = -(s + p^*)/(s + p^* + 1)$. The sublayer concentration $n_s(t)$ derived from Eq. 16, and the surface concentration evaluated from Eq. 17, are shown in Figs. 4 for various values of γ.

Let us estimate typical parameter values for viral fusion or molecular binding processes. Typical diffusion constants for viruses of diameter 100nm and in aqueous environments, are $D \sim 10^{-8}\mathrm{cm}^2/\mathrm{s}$. Using the typical screened electrostatic interaction potential, $\ell \approx 10^{-7}\mathrm{cm}$, we estimate the dimensionless diffusion coefficient $D \sim 10^6\mathrm{s}^{-1}/q_1$. On the other
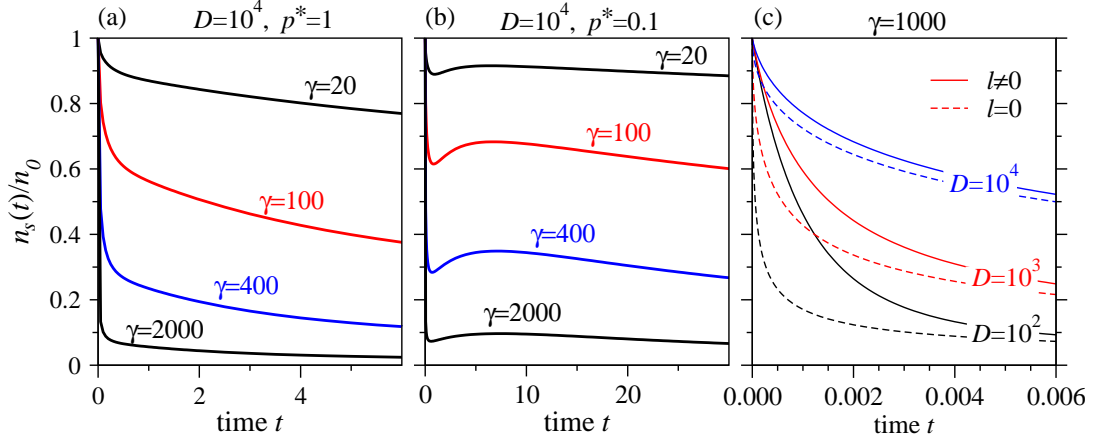
FIG. 4: Surface densities $n_s(t)$ for $N = 1$. (a) The sublayer density $n_s(t)$ as a function of time, for various values of the dimensionless adsorption rate γ. The other parameters are fixed at $D = 10^4$ and $p^* = 1$. (b) The sublayer density $n_s(t)$ for $D = 10^4$, and $p^* = 0.1$. Note the bump in concentration imparted by the slow annihilation rate p^*. (c) The deviation of $n_s(t)$ (for $\gamma = 1000$) if the transient term $\ell dn_s/dt$ is neglected. The solid curves are found from the full equation 13, while the dashed curves are solutions when the left-hand-side of Eq. 13 is neglected. The deviation occurs only at very short times, is independent of p^*, and is greatest for smaller diffusion coefficient D.

hand, typical diameters of small ligand molecules are of the order of 1nm yielding a nondimensional diffusion constant $D \sim 10^8 \text{s}^{-1}/q_1$. The nondimensional γ estimated using the thermal velocity v_T is now $\gamma \approx f v_T/(\ell q_1)$. For virus particles $\gamma \sim 10^8 \text{s}^{-1} f/q_1$, while for molecular ligands $\gamma \sim 10^{10} \text{s}^{-1} f/q_1$. The dissociation rate q_1 is highly variable and typically falls in the broad range $q_1 \sim 10^{-4} \text{ s}^{-1}$ to 10^4s^{-1}. For the gp120-CD4 interaction, the dissociation has been estimated in model systems [20] to be $q_1 \sim 10^{-3} \text{s}^{-1}$, while the detachment rate for mutant viral species [21] can be as high as $q_1 \sim 10^3 \text{s}^{-1}$. Lower dissociation rates are possible in tighter binding ligand receptor pairs such as EGF-receptor [28] where $q_1 \sim 10^{-4} \text{s}^{-1}$. For other pairs such as P-selectin and its receptors [29, 30], $q_1 \sim 0.1 \text{s}^{-1}$ to 1 s^{-1}. The sticking probability f is proportional to the binding probability of upon ligand-receptor contact, multiplied by the receptor area fraction at the interface. The factor f depends on the receptor density, but is typically of the order $f \sim 10^{-4} - 10^{-2}$.

In Fig. 4(a) we plot the sublayer density n_s as a function of time. For $p^* = 1$, Fig. 4(a) shows that the sublayer density $n_s(t)$ starts at its initial value n_0 and decreases with a nondimensional rate proportional to γ, eventually monotonically reaching $n_s(t \to \infty) \to 0$. If the annihilation rate p^* is decreased, n_s may no longer be monotonic. The observed increase in the surface concentration is due to the slow consumption of material at the interface, allowing some of the material to desorb after being delayed at the interface, rather than irreversibly reaching the final annihilated or fused state. For example,

when $p^* = 0.1$, the surface concentration $n_s(t)$ first decreases but recovers slightly at longer times, before ultimately decaying to zero as shown in Fig. 4(b).

Note that the curves for $n_s(t)$ exhibit a transient at short times determined by $1/\gamma$. Beyond this transient, the full solution we plot in Fig. 4(b) reduces to the outer solution, corresponding to setting $dn_s/dt = 0$ on the left hand side of Eq. 9. Fig. 4(c) explicitly shows different behaviors of the full and outer solutions during the transient time. The effect of the $\ell dn_s/dt$ term is to slow down the initial decrease of n_s, particularly for short times within the transient defined by $1/\gamma$. The effects of neglecting the boundary layer are less pronounced for larger bulk diffusivities D.

The temporal evolution of $n_s(t)$ is strongly dependent on $\Gamma_1(t)$. In fact, the nonmonotonicity of $n_s(t)$ for small p^* shown in Fig. 4(b) arises from the build-up of Γ_1 indicated in Fig. 5(a) which can get released back into the subsurface layer. For smaller p^*, Γ_1 reaches larger values. As long as $p^* > 0$, both n_s and Γ_1 vanish at sufficiently long times. Complete particle depletion near the surface occurs in dimensions less than two because there is no bounded steady-state solution to the diffusion equation and the depletion zone moves away from the interface for all times as shown in Fig. 5(b). Despite free diffusion, the bulk is unable to sustain a particle source near the surface as is known from classic diffusion theory [31]. The replenishment at small annihilation rates p^* also manifests itself in the bulk. In the case shown in Fig. 5(b), as time increases from $t = 0.75$ to $t = 6$, the bulk concentration near the interface recovers before
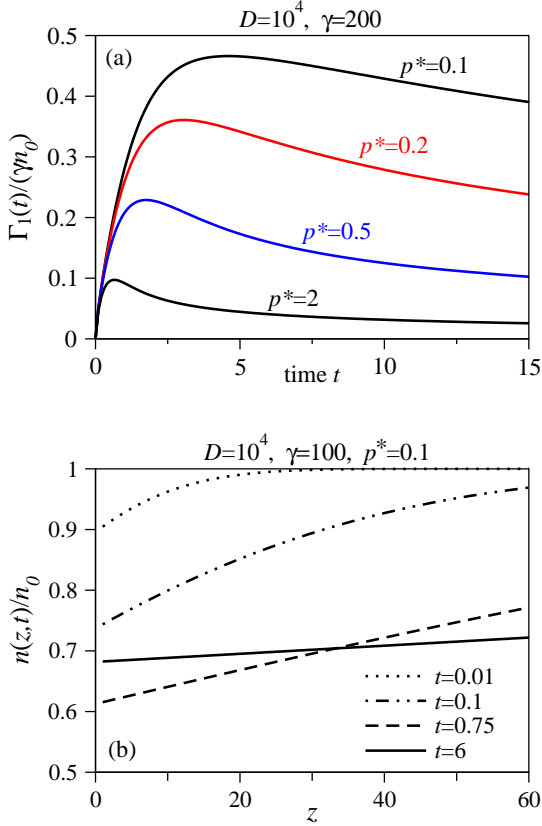
FIG. 5: (a) The surface concentration $\Gamma_1(t)$ for various p^* with $D = 10^4$ and $\gamma = 200$. (b) The bulk density profiles $n(z,t)$ as a function of position z at times $t = 0.01, 0.1, 0.75$, and 6.

FIG. 6: Dependence of surface quantities on number of steps N in the surface reaction scheme. (a) The sublayer density n_s as N is increased. The initial rapid fall from $n_s/n_0 = 1$ is imperceptible on this scale. (b) The surface concentrations Γ_i as a function of time for $N = 4$.

ultimately decreasing according to Eq. 21.

For general N, the eigenvectors and eigenvalues must be explicitly computed. In Fig. 6(a), we plot n_s as a function of N for uniform $q = 1$ and uniform p. For small p, the surface kinetics is a highly biased random walk away from Γ_N toward Γ_1, resulting in a larger n_s. Both small p and large N, hinder the annihilation process and impart a more reflective character to the interface. After initial transients, both n_s and the surface concentrations Γ_i maintain a high level for a long time before dissipating. Larger N also effectively trap surface material in the surface reservoir Γ_i. The relative amounts of Γ_i for $N = 4$ are shown in Fig. 6(b). For the small $p = 0.1$ used, most of the surface density lies in the initial species Γ_1, decreasing in the latter species.

V. SUMMARY AND CONCLUSIONS

We derived an effective, integro-differential equation for the boundary condition of a simple diffusion process. The approach presented differs from the typ-
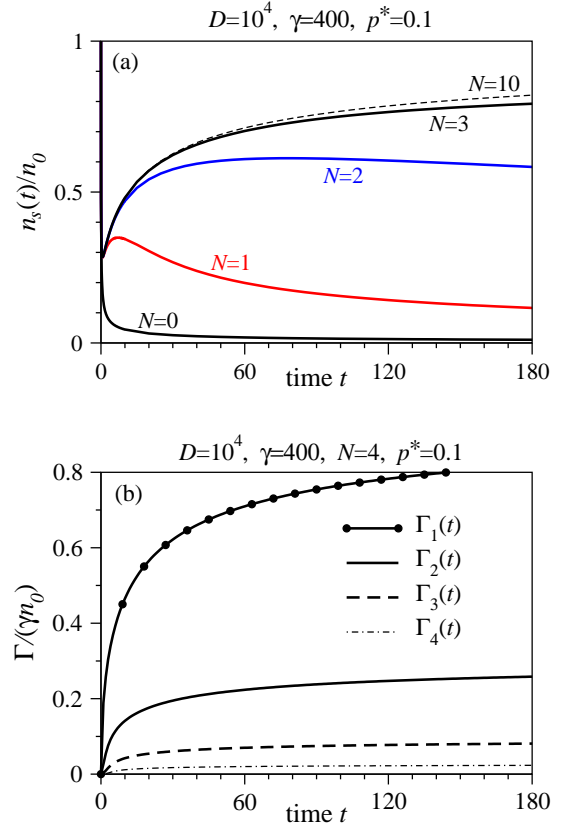
ical Ward and Tordai treatments since we use a linear model for the time rate of change of the initially adsorbed species Γ_1, rather than eliminating the bulk diffusion equation. The effects of intermediate chemical steps at the boundary are described by a delay kernel that can be decomposed using Laplace transforms. This kernel is an explicit function of the eigenvalues and eigenvectors of the surface reaction transition matrix. Our results suggest that measurement of a few quantities, such as fluorescence monitoring of the sublayer density [32], can be used to reconstruct the principal components of $K(t)$. This approach can be used to probe qualitative features of the surface kinetics important in modeling cell membrane signaling and viral infection, where a sequence of chemical steps at the surface are required before initiation of signaling or viral fusion. In HIV infection, the initial adsorption rate would be proportional to the surface CD4 concentration, and the subsequent rates in the reaction scheme in Fig. 2 would depend on the coreceptor concentrations, their surface mobilities, as well

as the effects of cooperative binding [18]. All of these physical attributes are encoded in the distribution of eigenvalues and eigenvectors of $\mathbf{M}$.

For simple linear reaction schemes on a flat surface, we find explicit dependences of the surface concentrations Γ_i and sublayer concentrations on the eigenvalues and eigenvectors of the transition matrix. For smaller annihilation rates p^*, and at least one ($N \geq 1$) surface intermediate, we find that the surface concentration persists and can replenish the bulk concentrations n_s after its initial decay. The depletion zone in the bulk can also recover. Delays that induce instabilities in dynamical systems have been well established [33]. Here, although the delay occurs in a boundary condition, we observe nonmonotonic behavior arising in the bulk concentrations as well. This rebounding effect is also apparent if one differentiates Eq. 9 with respect to time, giving a second order, harmonic oscillator-like equation, plus a dissipative coupling to the bulk concentration.

Whether the surface concentration or the bulk concentration near the surface vanishes at long times depends on the surface kinetics as well as geometry. If the combined surface kinetics towards annihilation is slow relative to bulk diffusion, the decay of the sublayer concentration n_s can be extremely slow. Similarly, if the number of surface states is large, there is an effective delay to annihilation and a higher probability that a surface species can detach and replenish the sublayer concentration. This effect is very sensitive to the annihilation rate p^* and the size of the reaction N and can keep the subsurface concentration high for essentially all times.

A number of extensions and related approaches to this and related systems can be readily investigated. For example, in applications such as surfactant adsorption, the surface concentration $\mathbf{\Gamma}$ can be appreciable and suppress additional adsorption. If surface species Γ_i has molecular area a_i, an adsorption term including steric exclusion would be $\gamma n_s(1 - \sum_{i=1}^{N} a_i \Gamma_i)$. The surface rate equations remain linear in $\mathbf{\Gamma}$, but with a time-dependent transition matrix $\mathbf{M}$. The effective boundary condition Eq. 9 is now nonlinear in $n_s(t)$ through $F[n_s]$. However, for many biochemical applications (such as cell signaling and virus adsorption and entry) the total surface concentration is low such that $\sum_{i=1}^{N} a_i \Gamma_i \ll 1$ and the adsorption term can be linearized. In our one-dimensional analysis, as long as N is not too large and there is an appreciable annihilation process, the surface concentrations all vanish in time.

The effects of multistage adsorption can also be explored on surfaces of arbitrary shape, particularly for cylinders and spheres. For multistage processes on a sphere, the sublayer concentration approaches a positive value $n_s(t \to \infty) = n_0(1 - \frac{\gamma K_0}{D + \gamma K_0})$. We also

expect positive eigenvalues $\lambda_j > 0$ of $\mathbf{M}$ to have a striking effect on the transport.

Finally, although we have only considered simple linearized surface reaction schemes with negative eigenvalues, systems that support oscillations, such as those involved in surface-mediated cell signalling, could also be treated within our framework. Features of the surface reactions and the bulk concentrations near the reacting surface remain coupled through the kernel $K(t)$. Under certain conditions, nonlinear surface reaction schemes may also be linearized. One example is in the *stochastic* representation of the surface reactions. If we write the surface quantities in terms of the probability distribution function $P(n_1, n_2, n_3, \ldots, t)$ that there are n_1 molecules of of type 1, n_2 of type 2, etc., the surface reactions can be written as a linear Master equation. This allows our approach to be applied when Γ_1 in the last term of Eq. 4 is interpreted as $\langle \Gamma_1(t) \rangle$, the ensemble average $\sum_{\{n_i\}} n_1 P(\{n_i\}, t)$. Using this interpretation, the full problem can be solved using linear methods similar to those presented, albeit for extremely large matrix dimension.

VI. APPENDIX

Here, we derive asymptotic expression for bulk and surface densities. The trivial short time behavior of the subsurface density is $n_s(t)/n_0 \sim (1-\gamma t)$, independent of the surface reactions since the first physical phenomenon to occur is particle adsorption from the bulk to the interface, at rate γ.

For large distances $(z - 1)/\sqrt{Dt} \gg 1$ and in the limit $\gamma \tilde{K}(s = 0) \equiv \gamma K_0 \gg \sqrt{D/t}$, asymptotic evaluation of the inverse Laplace inversion integral over $\tilde{n}(z, s)$ yields

$$\frac{n(z,t)}{n_0} \sim 1 - \left(1 + \frac{\sqrt{\pi D}}{\gamma K_0 \sqrt{t}}\right) \exp\left[-\frac{(z-1)^2}{4Dt}\right]. \tag{20}$$

The condition $\gamma K_0 \gg \sqrt{D/t}$ can be interpreted as a comparison between two typical velocities. The usual diffusive velocity, $\sqrt{D/t}$, is compared to an effective reaction velocity expressed by γ modulated by surface effects through the kernel K_0. We may thus define an effective Damköhler number $D_a \equiv \gamma K_0 \sqrt{t}/\sqrt{D}$, so that Eqn. 20 is valid only at large distances and for large values of D_a. The leading term on the right-hand-side above is independent of the surface kinet-

ics: the first information to have traveled away from the interface is the initial depletion of the n_s layer into the surface and interfacial effects emerge as first order corrections.

In the $t \to \infty$ limit, the dominant contribution to $n(z, t)$ comes from small values of u in Eq. 16. Approximating $L(1, u)$ with its $u \to 0$ limit, we find the asymptotic long time limit

$$
\begin{aligned}
n_s(t) \ &\sim \ \frac{n_0}{\gamma K_0} \sqrt{\frac{D}{\pi t}} \\
&\sim \ \frac{n_0}{\sqrt{t}} \left[\frac{\sqrt{D}}{\gamma \sqrt{\pi} \left(1 + \sum_{j=1}^{N} V_{1j}^{-1} V_{j1} \lambda_j^{-1} \right)} \right].
\end{aligned}
\tag{21}
$$

This expression is valid only if the surface dynamics include a net sink of material. As long as there is some annihilation, $K_0 = 1 + \sum_{j=1}^{N} V_{1j}^{-1} V_{j1}/\lambda_j < 0$ and Eq. 21 holds. A similar consideration of the small-u dominated integration in Eq. 17 yields for the surface concentrations

$$
\Gamma_k(|\lambda^*|t \to \infty) \sim \frac{n_0}{K_0} \sqrt{\frac{D}{\pi t}} \sum_{j=1}^{N} V_{kj}^{-1} V_{j1} |\lambda_j|^{-1}, \quad (22)
$$

where $\lambda_* < 0$ is the largest eigenvalue of the chemical transition matrix $\mathbf{M}$. Both Eq. 21 and 22 exhibit diffusion-limited $1/\sqrt{t}$ behavior. These general results rely only on the linearity of $F[n_s]$ and are valid for *any* surface reaction scheme through the eigenvalues and eigenvectors of the transition matrix $\mathbf{M}$ and the resulting function $\tilde{K}(s)$.

[1] A. F. H. Ward and L. Tordai. J. Chem. Phys. **14**, 453-461 (1946).
[2] H. Diamant, G. Ariel, and D. Andelman. Colloids and Surfaces A. **183-185**, 259-276 (2001).
[3] M. Mulqueen, K. J. Stebe, and D. Blankschtein, Langmuir **17**, 5196-5207 (2001).
[4] S.-Y. Lin, K. McKeigue, and C. Maldarelli, AIChE Journal **36**, 1785 - 1795 (1990).
[5] H. C. Berg and E. M. Purcell, Biophys. J. **20**, 193-219 (1977).
[6] C. W. Beverung, C. J. Radke, and H. W. Blanch, Biophysical Chemistry **81**, 59-80 (1999).
[7] C. Ybert and J. M. di Meglio, Langmuir **14**, 471-475 (1998).
[8] J. M. Schurr, Biophys. J. **10**, 700-716 (1970).
[9] J. M. Schurr, Biophys. J. **10**, 717-727 (1970).
[10] P. Bongrand, Rep. Prog. Phys. **62**. 921-968 (1999).
[11] S. J. Pogorzelski and A. D. Kogut, Oceanol. **43**, 389-404 (2001).
[12] D. A. Edwards, IMA Journal of Applied Mathematics, **63**, 89-112. (1999).
[13] J. Satulovsky, M. A. Carignano, and I. Szleifer, Proc. Natl. Acad. Sci. U.S.A. **97** 9037-9041 (2000).
[14] F. Fang, J. Satulovsky, and I. Szleifer, Biophys. J. **89**, 1516-1533 (2005).
[15] E. Leikina, I. Markovic, L. V. Chernomordik, and M. M. Kozlov, Biophys. J. **79**, 1415-1427 (2000).
[16] M. J. Clague, C. Schoch, and R. Blumenthal, J. Virology **65**, 2402-2407 (1991).
[17] *Viral Fusion Mechanics* edited by J. Bentz (CRC Press, Boca Raton FL, 1993)
[18] S. E. Kuhmann, E. J. Platt, S. L. Kozak, and D. Kabat, J. Virology **74**, 7005-7015 (2000).
[19] E. J. Platt, J. P. Durnin, and D. Kabat, J. Virology **79**, 4347-4356 (2005).
[20] D. G. Myszka, R. W. Sweet, P. Hensley, M. Brigham-Burke, P. D. Kwong, W. A. Hendrickson, R. Wyatt, J. Sodroski, and M. L. Doyle, Proc. Natl. Acad. Sci. USA. **97**, 9026-9031 (2000).
[21] H. Wu, D. G. Myszka, S. W. Tendian, C. G. Brouillette, R. W. Sweet, I. M. Chaiken, and W. A. Hendrickson, Proc. Natl. Acad. Sci. U.S.A. **93**, 15030-15035 (1996).
[22] Y. J. Kwon, G. Hung, W. F. Anderson, C. A. Peng, and H. Yu, J. Virology **77**, 5712-5720 (2003).
[23] M. Gopalakrishnan, K. Forsten-Williams, T. R. Cassino, L. Padro, T. E. Ryan, and U. C. Tauber, *Eur. Biophys. J.*, **34**, 943-958, (2005).
[24] E. M. Lifshitz and L. P. Pitaevskii, *Physical Kinetics*, (Pergamon Press, 2002).
[25] L. S. Jung and C. T. Campbell, Phys. Rev. Lett. **84**, 5164-5167 (2000).
[26] P. Kisliuk, J. Phys. Chem. Solids **5**, 78-84 (1958).
[27] M. P. McGee, and T. Chou, J. Biol. Chem. **276**, 7827-7835, (2001).
[28] K. Maeda, Y. Kato, and Y. Sugiyama, J. Controlled Release **82**, 71-82 (2002).
[29] J. Fritz, A. G. Katopodis, F. Kolbinger, and D. Anselmetti, Proc. Natl. Acad. Sci. USA. **95**, 12283-12288 (1998).
[30] R. Alon, D. A. Hammer, and T. A. Springer, Nature **376**, 539-542 (1995).
[31] J. Crank, *The Mathematics of Diffusion* (Oxford University Press, Oxford, 1975).
[32] A. M. Lieto, R. C. Cush, and N. L. Thompson, Biophys. J. **85**, 3294-3302 (2003).
[33] N. MacDonald, *Biological delay systems: linear stability theory* (Cambridge University Press, Cambridge, 1989).